American Mineralogist, Volume 84, pages 639–649, 1999

Properties of As and S at NiAs, NiS, and $Fe_{1-x}S$ surfaces, and reactivity of niccolite in air and water

H. WAYNE NESBITT* AND M. REINKE

Department of Earth Sciences, University of Western Ontario, London, Ontario, Canada N6A 5B7

ABSTRACT

Niccolite (NiAs), NiS (high temperature form), and pyrrhotite ($Fe_{1-x}S$) are structurally related, with sulfur and arsenic sixfold coordinated. Their fracture or cleavage necessarily produces surface As and S species of lower coordination. Some sp^3 hybridized As and S ions likely form at these surfaces, as observed for As at GaAs and S at pyrite surfaces. Upon relaxation, lone pairs of electrons occupy As and S dangling bonds, with the lone pair directed away from the surface and poised to react with adsorbates. According to the valence shell electron pair repulsion (VSEPR) model, the lone pair should repel the three hybrid orbitals forming metal-As or metal-S bonds, causing tetrahedral angles to contract and As and S ions to "protrude" from the surface.

X-ray photoelectron spectroscopic (XPS) study of niccolite (NiAs) surfaces fractured under high vacuum (10^{-9} torr) indicate that arsenic is more reactive than Ni toward residual gases of the XPS analytical chamber, as evident from development of small As^{1+} and As^{3+} photopeaks in the As(3d) XPS spectrum. Hydroxide observed in the O(1s) XPS spectrum suggests formation of $As(OH)_3$. The O(1s) spectrum also revealed adsorbed H_2O and atomic oxygen radical (produced by dissociation of O_2) at the NiAs surface. Initiation of arsenic oxidation probably involved reduction of adsorbed atomic oxygen radicals, followed by hydration to produce hydroxyl, and finally to produce the observed $As(OH)_3$ surface species. There was no evidence for Ni reaction with residual gases.

Reaction of NiAs with air over 30 h yields a thin (~10 Å) oxidized overlayer containing $Ni(OH)_2$, arsenite, and arsenate. Similarly thin oxidized layers, composed of oxyhydroxides and sulfates, are produced on millerite and pyrrhotite surfaces. All three surfaces are largely passivated toward air after only a few hours reaction.

A thicker oxidized overlayer (~120 Å thick) containing the same secondary products as the air-ixidized surface is produced on NiAs after 7 days reaction with aerated, distilled water. The accumulation of arsenite and arsenate salts at the niccolite surface distinguishes it from millerite and pyrrhotite surfaces reacted with aerated solutions. Ni- and Fe-sulfate salts produced from these latter two minerals are highly soluble, hence do no accumulate at the mineral surfaces whereas Ni-arsenate (and apparently Ni-atsenite) salts are less soluble and accumulate on oxidized niccolite surfaces along with $Ni(OH)_2$.

INTRODUCTION

Detailed surface studies of minerals such as pyrrhotite, pyrite, and niccolite are hampered by their propensity to fracture rather than cleave along preferred crystallographic orientations. Natural fracture surfaces display steps and defects, are rough, and generally not amenable to study by surface-sensitive structural techniques (e.g., low energy electron diffraction). Even techniques such as X-ray photoelectron spectroscopic (XPS) and auger electron spectroscopy (AES) are hindered because unpredictable crystallographic orientations, exposed during fracture, lead to "averaged" surface properties. It is precisely these fracture surfaces, however, that are exposed in natural settings in sedimentary environments (through abrasion and comminution), during milling of ores in preparation for flotation, and in tailings and waste dumps of mining operations. It is therefore critical to document these "averaged" properties, and to deduce reaction mechanisms if natural and industrial processes are to be better understood.

The inability to obtain oriented pristine surfaces increases the importance of studies of allied compounds that can be cleaved along specific crystallographic planes. Various cleavage surfaces of GaAs (zincblende structure), for example, have been studied. Surface states of both Ga and As exist on GaAs {110} surfaces, with surface relaxation achieved by outward protrusion of As from, and collapse of Ga toward, the bulk (Eastman et al. 1980; Smit and van der Veen 1986). Reconstruction of the GaAs {100} and other surfaces results in formation of As dimers and trimers (Pashley et al. 1988; Biegelsen et al. 1990a). Minerals of the NiAs structure (or derivatives) with poor or no cleavage are expected to display all these features.

The structures of numerous minerals, including the pyrrhotites, can be derived through distortion and transformation of the niccolite hexagonal structure (Kjekshus and Pearson 1964; Vaughan and Craig 1978). A better understanding of NiAs surface properties should provide insight into the properties of all

*E-mail: hwn@Julian.uwo.ca

0003-004X/99/0004–0639$05.00

minerals with related structures. The first part of this study reports the findings of an XPS and Auger study of a "pristine," NiAs surface, the surface properties of As at fracture surfaces, and incipient oxidation of this surface to obtain greater insight into the surface properties and reactivity of minerals with this structure. The second part uses AES to investigate the composition and thickness of oxidized surface layers developed on NiAs reacted with air and aerated, distilled water, discusses the nature of the reactions that have occurred at the surface of niccolite, NiS, and pyrrhotite surfaces. The discussion draws heavily on previous studies of III-V semiconductors (e.g., GaAs) to interpret the surface analytical results.

EXPERIMENTAL METHODS

Samples and instrumentation

NiAs from the Cobalt area of Northern Ontario was obtained from the University of Western Ontario Suffel collection (sample number 6983). Precise sample location and collection date are unknown. Niccolite has no preferred cleavage and typically fractures concoidally. Standard polished thin sections were prepared and the mineral was characterized by optical reflected-light microscopy, X-ray diffraction, scanning electron microscopy, and electron microprobe.

AES and XPS studies were conducted on specimens cut by a diamond saw into 2 mm × 3 mm × 10 mm parallelopipeds. Specimens displaying macroscopic or microscopic fractures, or inclusions were discarded. The remaining samples were cleaned in acetone, dried and stored in a low vacuum desiccator. One parallelepiped was introduced to, and fractured in, the XPS analytical chamber to expose a pristine fracture surface, from which were collected XPS spectra. Other parallelopipeds were fractured under nitrogen and the fracture surfaces allowed to react with the atmosphere or distilled, deionized water for various periods. The reacted fracture surfaces were transferred to the XPS and AES instruments in a nitrogen-filled glove bag. The experiments were conducted under ambient laboratory conditions, where the temperature ranged between 22 and 24 °C, with humidity ranging from 60 to 90%.

A modified Surface Science Laboratories SSX-100 XPS instrument with monochromatized Al$K\alpha$ X-ray source and analytical chamber base pressure of 1×10^{-7} Pa was used to collect all XPS spectra. The spectrometer work function was adjusted to 84.00 eV for the Au ($4f_{7/2}$) photopeak and energy dispersion was set to yield an energy difference of 857.5 eV between the Cu($2p_{3/2}$) and Cu(3p) lines. No charge corrections were required. Survey scans were collected using a 600 μm spot size and a fixed pass energy of 160 eV. Narrow scans were recorded using a 600 μm spot size and a fixed pass energy of 50 eV.

Auger spectra were obtained with a Perkin-Elmer PHI 600 scanning Auger microprobe with an SEM detector and an Ar sputter gun. Analytical chamber base pressure was 10^{-7} Pa whereas pressures during sputtering were near 10^{-6} Pa. Survey scans were collected with an electron beam acceleration potential of 5.0 kV at a current of 60–75 nA. The beam was focused to about 1 μm with the cylindrical mirror analyzer resolution set to 1.2%. Depth profiles were collected by rastering a 30° incident 2.0 kV Ar^+ beam over a 2 mm × 2 mm surface area. Profiles were collected as a function of time and converted to depth by assuming the sputter rate of NiAs to be similar to that of pyrrhotite, at about 40 Å/min (Pratt et al. 1994a).

NiAs characterization

Twenty-two microprobe analyses yielded an average composition, Ni = 49.15% (±0.20), As = 50.85% (±0.20), Fe = 0.01% (±0.04), Co = 0.20% (±0.20), and S = 0.01% (±0.20).

XPS broadscan results of the vacuum-fractured surface yielded 22.6% (atomic) As [As(3d) line], 18.3% Ni [Ni(3p) line], 8.6% O [O(1s) line], and 50.5% C [C(1s) line] using peak areas and theoretical cross sections (Scofield 1976). Oxygen is low on the surface but (adventitious) carbon is high. Sulfur was detected at the surface although it should not have been, at the levels indicated by the electron microprobe analysis. It may be present in small inclusions but more likely it accumulated in the near-surface as a result of fracture. If present as very small inclusions, they must be millerite (NiS) because only Ni was detected by XPS. The XPS narrow scans of pristine NiAs, air and water reacted NiAs surfaces are illustrated, respectively, in Figures 1, 2, and 3.

XPS fitting procedures

Raw counts are plotted on the ordinate of each XPS diagram as an aid to evaluation of counting statistics. The atomic oxygen on the vacuum-fractured surface (Fig. 1d), for example, has an associated error of about 20% whereas the OH^- contribution to the air-reacted surface (Fig. 2c) has about 5% error. Errors associated with the major Ni and As peaks of Figure 1 are about 1 to 2%. None of the spectra was smoothed.

Peak shape. Niccolite is a conductor (Vaughan and Craig 1978) and conductors yield asymmetric peaks due to interaction of photoelectrons with electrons of the conduction band. Doniach and Sunjic (1970) explained the effect and provided an expression with which to fit these asymmetric peaks. As for millerite spectra (Legrand et al. 1998), photopeaks of all elements here investigated are asymmetric and were consequently fitted with a Gaussian-Lorentzian peak shape with a Doniach-Sunjic high energy tail (Briggs and Seah 1990, Appendix 3).

Ni($2p_{3/2}$) peaks. The substantial similarities between NiS and NiAs Ni(2p) spectra allow Ni(2p) spectral fits of pristine and reacted millerite (Legrand et al. 1998) to be used as guides to fit Ni(2p) XPS spectra of pristine and reacted NiAs surfaces. Each Ni(2p) contribution consists of two peaks (Legrand et al. 1998), a main peak near 853 eV, and a broad, low intensity satellite peak located at about 860 eV (Figs. 1a, 2a, and 3a). The fit parameters for the Ni($2p_{3/2}$) peaks of NiAs evaluated from Figure 1a in Table 1, are almost identical to the Ni(2p) parameters for pristine NiS. The peak parameters for $Ni(OH)_2$ of reacted surfaces (Figs. 2a and 3a) were taken from Legrand et al. (1998). Legrand et al. (1998) identified a $NiSO_4$ contribution to reacted NiS surfaces and there is an equivalent contribution to the Ni(2p) spectrum of reacted NiAs. This contribution, however, may be derived from Ni bonded to arsenite and to arsenate (Figs. 2a and 3a); the As(3d) spectra of reacted surfaces indicate both arsenite and arsenate (Figs. 2b and 3b). Inspection of the Ni(2p) spectra indicates that there is no justification for introduction of a peak for each contribution; consequently, one broad peak near 857 eV, with a satellite near

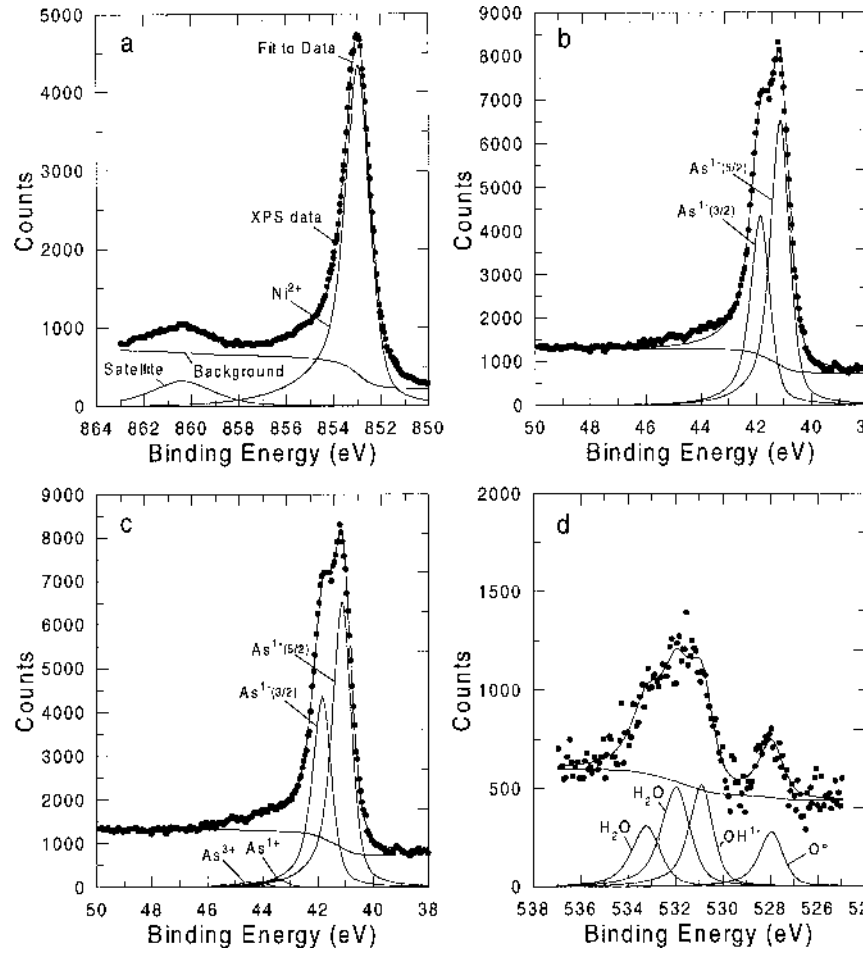

▶ **FIGURE 1.** Narrow scan XPS spectra of a NiAs surface fractured in the vacuum of the analytical chamber of the XPS instrument pots, data points. Solid lines = component peaks and their summation. (**a**) The Ni($2p_{1/2}$) spectrum of niccolite. Backgrounds is indicated as labeled. The major peak is Ni bonded to As (labeled Ni^{2+}). The broad low intensity peak is a satellite of the major peak. (**b**) The As(3d) spectrum of unreacted NiAs. The fit includes only the As^{1-} contribution. There is a poor fit in the region between 43 and 45 eV. (**c**) Same as part **b** but small contributions from As^{1+} and As^{3+} have been added to improve the fit in the 43 to 45 eV range. (**d**) The O(1s) spectrum of the unreacted NiAs surface. The O is acquired from the residual gases of the analytical chamber, thus explaining the low counts. O°, OH^{-}, and H_2O represent, respectively, atomic oxygen, hydroxide, and two forms of water, probably chemisorbed and physisorbed (physisorbed H_2O peak located at higher binding energy; Knipe et al. 1995).

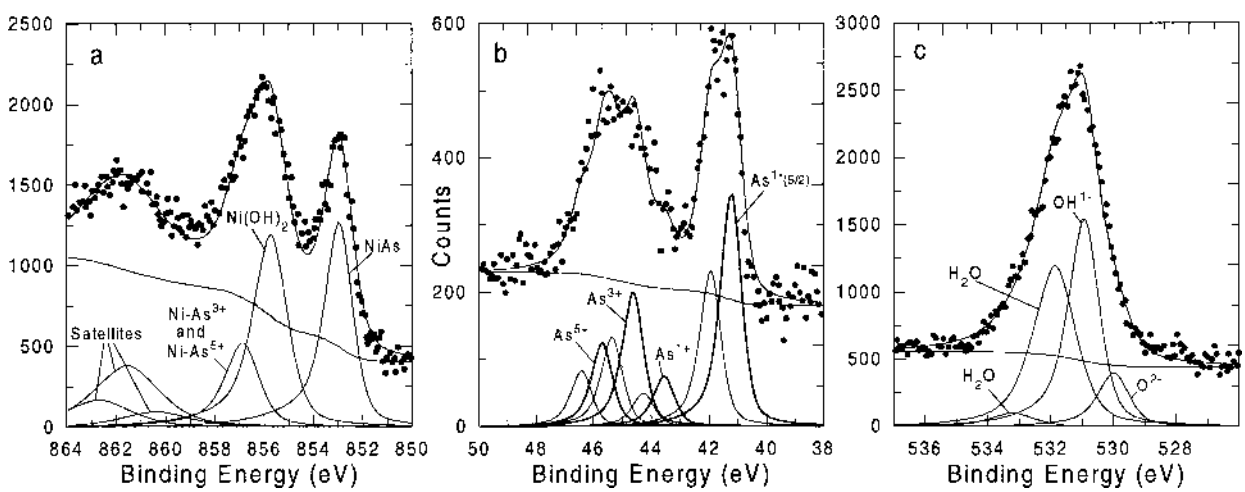

▲ **FIGURE 2.** Narrow scan XPS spectra of a NiAs surface reacted with air for 30 h. Symbols as in Figure 1. (**a**) The Ni($2p_{1/2}$) spectrum showing Ni bonded to As (NiAs), to hydroxide (Ni[$OH]_2$), arsenite (Ni-As^{3+}), and arsenate (Ni-As^{5+}). (**b**) The As(3d) spectrum of 30 h air-reacted NiAs. Five As oxidation states are considered, and required to produce a good fit. Each As($3d_{5/2}$) peak is labeled and is drawn with slightly thicker lines than the associated As($3d_{3/2}$) peaks. The unlabelled peaks are As($3d_{3/2}$) peaks and the contribution of each is calculated entirely from the associated As($3d_{5/2}$) peak (they are not fitted). (**c**) The O(1s) spectrum with peaks labeled as in Figure 1d. The O^{2-}, OH^{1-}, and H_2O labels indicate oxide, hydroxide O, and O of water. There are two very broad H_2O peaks. Their nature is uncertain, although the low binding energy for the major peak suggests chemisorbed water (Knipe et al. 1995).

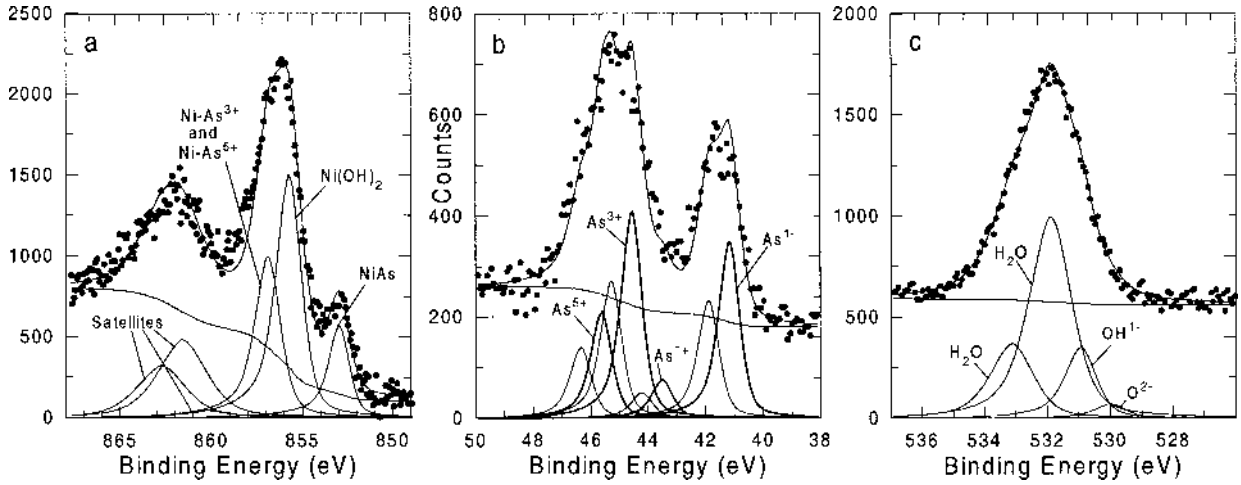

FIGURE 3. Narrow scan XPS spectra of a NiAs surface reacted with aerated, distilled, and deionized water for 7 d. Symbols as in Figure 1. (**a**) The Ni($2p_{1/2}$) spectrum. The species observed in Figure 2a are present, in different proportions, at the water reacted surface. (**b**) The As(3d) spectrum. The species are the same as found at the air reacted surface (Fig. 2b). (**c**) The O(1s) spectrum with peaks labeled as in Figure 1d. The lower binding energy H_2O peak is interpreted to be chemisorbed water and the higher binding energy peak is considered to be physisorbed water

863 eV (Table 1) was used to fit the two contributions. The peak parameters for the Ni-arsenite and Ni-arsenate contributions are similar to those for the Ni-SO_4 contribution to reacted NiS (Legrand et al. 1998). Additional study is required to determine if the binding energy of Ni bonded to arsenite is somewhat different from that of Ni bonded to arsenate.

As(3d) peaks. Each As(3d) XPS spectral contribution consists of a spin-orbit-split doublet, including a As($3d_{5/2}$) and a As($3d_{3/2}$) line. Peak parameters of all As($3d_{5/2}$) lines were evaluated from the XPS spectrum of Figure 1b but all peak parameters of the associated As^{1-}($3d_{3/2}$) peak were calculated as follows. The As($3d_{3/2}$) intensity was constrained to two-thirds that of the associated As($3d_{5/2}$) line, as required by theory. The full width at half maximum (FWHM) was assigned the same value for both peaks. The As($3d_{3/2}$) line was situated at 0.7 eV higher binding energy than the As($3d_{5/2}$) peak. Each As contribution (e.g., As^{3+}, As^{5+}) necessitates the introduction of both the 5/2 and 3/2 peaks, but the properties of the 3/2 peak are in each case calculated from those of the 5/2 peak. A Doniach-Sunjic contribution is required to complete the fit. The parameters in Table 1 represent the values that provide the best fit to the high energy portion of the peak in Figure 1b. These values were applied to fit the As spectra of the reacted surfaces (Figs. 2b and 3b).

TABLE 1. XPS spectral peak fitting parameters

Species	B.E. (eV)	FWHM (eV)	Treatment Pristine (At%)	Air (At%)	Water (At%)	Notes
Ni-As	853.0	1.20	91.3	28.2	10.3	Bulk Signal
Ni-As Satellite	860.5	3.20	8.7	4.3	1.8	Bulk Signal
Ni-OH	855.8	1.60		30.5	32.9	Surface Signal
Ni-OH Satellite	861.7	3.20		16.8	20.1	Surface Signal
$Ni\text{-}As^{3+}$-As^{5+}	856.9	1.60		13.0	21.8	Surface Signal
$Ni\text{-}As^{3+}$-As^{5+}	862.8	3.20		7.2	13.2	Surface Signal
As^{1-}	41.1	0.85	95.6	46.3	33.4	Bulk Signal
As^{1+}	43.5	0.85	2.6	10.2	7.3	Surface Signal
As^{3+}	44.5	0.85	1.8	26.8	39.3	Arsenite
As^{5+}	45.6	0.85		16.7	20.0	Arsenate
O°	528.0	1.15	15.7			Atomic Oxygen
O^{2-}	530.0	1.15		11.5	3.2	Oxide
OH^-	530.9	1.15	29.5	43.2	16.3	Hydroxide
H_2O	532.0	1.60	34.2	41.8	59.0	Chemisorbed
H_2O	533.3	1.60	20.6	3.5	21.5	Physisorbed

Notes: All peaks fitted as 60% Gaussian, 40% Lorentzian, and 30% asymmetry. Exponential factors of the Doniach-Sunjic contribution were 0.60, 1.30, and 0.90, respectively, for Ni, As, and O fits (Briggs and Seah 1990, Appendix 3). B.E. = binding engergy; Pristine = vacuum fractured surface; Air = surface reacted with air for 30 h; Water = surface reacted with aereated water for 7 d.

O(1s) peaks. The O signal on pristine niccolite is weak, but suggests a contribution at 528 eV, and numerous contributions at higher binding energy, including hydroxide and H_2O contributions. Ambiguity is associated with the water contributions. Knipe et al. (1995) demonstrated that H_2O may be very weakly to strongly bound to the surface and that it is difficult to distinguish among bonded H_2O of bulk phase, and chemisorbed, physisorbed, and H_2O "condensed" on the surface. The two H_2O peaks in the O(1s) XPS spectra are here arbitrarily assigned "chemisorbed" and "physisorbed" (Table 1). The various forms of H_2O are, however, given no additional consideration as they are not the focus of this communication.

Auger fitting procedures

Auger depth profiles of reacted NiAs were collected to a depth where Ni/As ratios no longer changed (e.g., Fig. 4a). The deepest 8 Auger analyses of each Auger depth profile were averaged and an empirical sensitivity factor for As determined to yield the Ni/As ratio of niccolite obtained from the averaged electron microprobe analyses. The empirical sensitivity factor was then applied to individual analyses of that profile. The procedure was repeated for each profile. The errors associated with individual analyses is about 5%, and this is apparent by com-

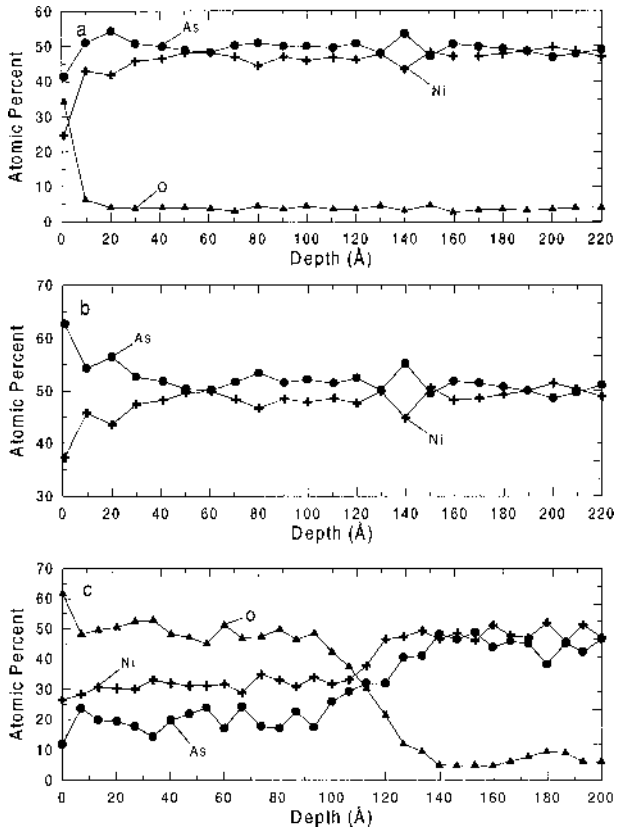

FIGURE 4. Auger compositional depth profiles of reacted NiAs surfaces. (**a**) Depth profile of 30 h air-reacted surface in which Ni, As and O normalized to 100%. The oxidized overlayer is less than 10 Å thick. (**b**) Depth profile of 30 h air-reacted surface in which only Ni and As have been normalized to 100%. As is preferentially enriched in the near-surface, apparently a response to surface oxidation. (**c**) Depth profile of 7 d water-reacted surface in which Ni, As, and O normalized to 100%. The oxidized overlayer is of near-constant composition. The depth profiles were collected as a function of time. Rate of sputtering was considered to be 40 Å/min, the same as for pyrrhotite (Pratt et al. 1994). The more massive nature, and high density of NiAs, implies that the depths represent maxima (e.g., oxidized overlayer is a maximum of 120 Å thick).

paring the variation in analytical results for Ni, As, and O for the deepest 8 analyses of each profile (Figs. 4a and 4c).

INTERPRETATION OF XPS SPECTRA

Vacuum-fractured surface

Ni($2p_{3/2}$) spectrum. A major, narrow peak at 853.0 (±0.2) eV (Fig. 1a; Table 1) is close to that of the Ni($2p_{3/2}$) peak of NiS (853.1 eV, Legrand et al. 1998). There is a broad, low intensity satellite peak centered at about 860.5 eV, as there is in the millerite Ni(2p) spectrum (centered at 859.7 eV).

Although the Ni(2p) spectral similarity in NiAs and NiS suggests similar Ni chemical states, this is not obvious from close inspection. The formal valence of Ni in millerite is 2+ but its formal valence in NiAs is uncertain. As shown subsequently, As of NiAs has a binding energy identical to As of arsenopyrite in which As is formally As^{1-}, implying a formal valence of 1+ for Ni. The electronegativities of Ni and As are similar whereas those of Ni and S are appreciably different (Allred 1961; Allred and Rochow 1958) and the ambiguity may result from the much greater covalency of NiAs compared with NiS. These aspects will be addressed elsewhere. To maintain continuity with millerite studies, the peak at 853.0 eV is referred to formally as Ni^{2+}. Peak fit parameters are provided in Table 1.

The major Ni(2p) peak of niccolite is asymmetric toward its high binding energy side, just as observed for millerite (Legrand et al. 1998), and it arises from interaction of emitted photoelectrons with conduction band electrons (Doniach and Sunjic 1970).

There is no evidence for any other surface contribution in the Ni(2p) spectrum, including Ni-oxygen bonds. A peak developed at 856 eV on air-oxidized NiAs (Fig. 2a) and NiS (Legrand et al. 1998) surfaces but this peak is not apparent on the vacuum-fractured surface, hence $Ni(OH)_2$ surface species are absent. Neither does evidence exist for Ni^{3+}, the Ni(2p) peak of which is located at binding energies 1.5 to 2 eV greater than observed for Ni^{2+} (Briggs and Seah 1990; Appendix 5, compare NiO and Ni_2O_3).

As(3d) spectrum. The As(3d) spectrum of niccolite (Fig. 1b) includes a strong doublet peak resulting from spin-orbit splitting. The As($3d_{5/2}$) contribution is located at 41.1 eV (±0.2 eV) and the As($3d_{3/2}$) contribution at 41.8 eV (see section on Fitting Procedures). The fitted peak parameters (Table 1) are effectively the same as observed for the As(3d) doublet in arsenopyrite (41.2 and 41.9 eV; Nesbitt et al. 1995). There is a high energy "Doniach-Sunjic" tail associated with each As peak (Fig. 1b and Doniach and Sunjic 1970), just as there is for S(2p) peaks of conductors NiS and Cu_2S (Legrand et al. 1998; Laajalehto et al. 1996).

A small contribution to the As(3d) spectrum is apparent in Figure 1b between 41.5 and 45.5 eV. Air-oxidized arsenopyrite surfaces (Nesbitt et al. 1995) display doublet peaks of As^{1+} and As^{3+} (bonded to O) located within this binding energy range, and As^{1+} doublet fitted at 43.5 ($3d_{5/2}$ peak) eV, and the As^{3+} doublet fitted at 44.5 eV ($3d_{5/2}$ peak) produces an excellent fit (Fig. 1c). The As^{1+} and As^{3+} doublets account for 2.6 and 1.8%, respectively, of the total As signal. Peak parameters are given in Table 1.

The energy of the photon source is 1486 eV thus approximately 8 NiAs monolayers were sampled (Seah and Dench 1779). As of the surface-most monolayer should contribute a minimum of 12% to the total As counts (and more because the signal of the surface-most layer is unattenuated). The 4.4% of oxidized As consequently represents less than monolayer coverage, indicating that oxidation has occurred at specific sites on the surface. As^{5+} is located near 45.6 eV ($3d_{5/2}$ peak) on the air- and water-reacted surfaces (Figs. 2b and 3b) but there is no evidence for such a contribution in Figure 1c. Apparently, oxidation produced only intermediate oxidation states. This may result from a low oxidation potential at the mineral-vacuum interface (oxidation potential too low to allow for full oxidation) or As^{5+} production may be too slow to be detected under these conditions.

O(1s) Spectrum. The broadscan analysis of the vacuum-fractured niccolite surface yields 7.8% O. The low count rate of the O(1s) narrow scan (Fig. 1d) indicates low O content and probably less than monolayer coverage. The peak at 528.0 eV (Fig. 1d) can be fitted with a FWHM of 1.15 eV, suggesting a contribution from a single surface species. The binding energy is exceptionally low for oxide (O^{2-}), which typically ranges between 529 and 531 eV (Briggs and Seah 1990; Pratt et al. 1994a, 1994b; Nesbitt et al. 1995; Legrand et al. 1998). The binding energy is, however, similar to that obtained by Barteau and Madix (1984) for atomic oxygen (O°) adsorbed to metallic silver and copper surfaces (528.3 eV). This peak is consequently interpreted to represent adsorbed atomic oxygen derived from the residual gases of the analytical chamber (discussed subsequently).

The major peak is very broad, extending from about 530 to 535 eV, thus includes numerous contributions. The O(1s) spectrum of air-reacted arsenopyrite was used as a guide to deconvolute the peak, and it is best fitted using hydroxide, chemisorbed, and physisorbed H_2O with respective binding energies of 530.9, 532.1, and 533.3 eV. As with arsenopyrite, the FWHM of the hydroxide peak is narrow (1.15 eV), but those of the two H_2O peaks are broad (1.6 eV) for reasons explained by Nesbitt et al. (1995) and Knipe et al. (1995).

There is no indication that hydroxide is bonded to Ni, in that there is no Ni-OH peak at 855.8 eV in the Ni(2p) spectrum of Figure 1a, although it is present on the air-reacted sample (Fig. 2a). Arsenic, however, shows evidence for oxidation (Fig. 1c) to As^{1+} and As^{3+}. The latter, when bonded to hydroxyl groups forms arsenite. Apparently hydroxide of the O(1s) peak is associated primarily with As.

Air- and water-reacted surfaces

Ni(2p) spectrum. Comparison of the 30 h air-oxidized (Fig. 2a) and vacuum-fractured surfaces (Fig. 1a) reveals development of a strong peak near 856 eV, and enhancement of the satellite peak centered at 861.7 eV, through reaction with air. Previous studies report a peak for Ni^{3+}-oxide at around 855.6 eV (Mansour and Melendres 1996a, 1996b), and a peak for Ni^{2+} bonded to OH^- at 855.6 to 856.2 eV (Legrand et al. 1998; McIntyre and Cook 1975; Mansour 1996a). As Ni^{3+} is not stable under natural conditions (produced only with strong oxidants) the peak at 855.8 is interpreted as a $Ni(OH)_2$ surface species, as observed on millerite surfaces. There may be a small Ni-O contribution near 854 eV (Mansour 1996b) as the fit deviates slightly from the XPS data in this region.

The peak near 856 eV is asymmetric and broad, suggesting it is composite. A similar composite peak was observed on air-oxidized NiS (millerite) surfaces where the two contributions were identified as $Ni(OH)_2$ (855.8 eV) and $NiSO_4$ (856.7 eV) surface species (Legrand et al. 1998). The 856 eV peak of Figure 2b is, by analogy, interpreted to include a $Ni(OH)_2$ and a Ni-arsenite/arsenate contribution at 856.9 eV (Fig. 2b demonstrates the presence of both As species). The surface properties of air-oxidized millerite and niccolite apparently are analogous with regards to their Ni(2p) spectra.

The NiAs surface reacted for 7 d with aerated, distilled water (Fig. 3a) displays the same contributions as the air oxidized NiAs surface, with each contribution at precisely the same binding energy (Table 1). The Ni-As signal (853.0 eV) is, however, greatly diminished in Figure 3a compared with Figure 2a. Relative to the $Ni(OH)_2$ peak (855.8 eV), the peak at 856.9 eV is proportionally more intense on the water-reacted surface than on the air-oxidized surface (compare Figs. 2a and 3a). An additional contribution may occur between 857 and 859 eV as the fit is poor in this region.

As(3d) Spectrum. The As(3d) spectrum of the 30 h air-oxidized sample (Fig. 2b) contains a peak centered at 41.1 eV representing As^{1-} of bulk niccolite (compare with Fig. 1c). The broad peak centered at 45 eV (Fig. 2b) is absent from the vacuum-fractured spectrum (Fig. 1c) but is similar to that of the As(3d) air-oxidized spectrum of arsenopyrite (Nesbitt et al. 1995). It is interpreted to result from As^{3+} and As^{5+} contributions [$As(3d_{5/2})$ and $As(3d_{3/2})$ signals from each]. A small peak near 43.5 eV, attributed to As^{1+}, was required to accurately fit both the air-reacted (Fig. 2b) and the vacuum-fractured spectrum (Fig. 1c, Table 1), as well as the air-oxidized arsenopyrite spectrum (Nesbitt et al. 1995).

The As(3d) spectrum of NiAs reacted for 7 d with aerated, distilled water (Fig. 3b) is similar to that reacted with air (Fig. 2c) except that the As^{3+} and As^{5+} signals are more intense in the former spectrum. The peak parameters used to fit both spectra (Figs. 2c and 3b) are identical (Table 1).

O(1s) Spectrum. The O(1s) spectrum of air-oxidized arsenopyrite (Nesbitt et al. 1995) was used as a guide to fit the O(1s) spectrum of NiAs (Fig. 2c). The spectrum is well fitted with three major contributions, oxide (530.0 eV), hydroxide (530.9 eV), and (chemisorbed) water at 532.0 eV (Table 1). A small amount of physisorbed water (3.5%) has been included in the fit (533.3 eV) but its abundance is uncertain as it is a region of strong Doniach-Sunjic contribution. The same major peaks were observed on air-reacted arsenopyrite surfaces (Nesbitt et al. 1995).

The O(1s) spectrum of the water-reacted surface (Fig. 3c) indicates the same species on both the water-reacted and air-oxidized surfaces (Fig. 2c). They include oxide (O^{2-}), hydroxide (OH^-), chemisorbed and physisorbed H_2O. Whereas OH^- is the dominant species on the air-oxidized surface, chemisorbed H_2O is the dominant species on the water reacted surface. Physisorbed water has increased substantially on the water reacted surface but O^{2-}/OH^- is similar on both surfaces. Proportions of species are shown in Table 1.

INTERPRETATION OF AES COMPOSITIONAL DEPTH PROFILES

Air-oxidized surface

The O signal of the Auger compositional depth profile (Fig. 4a) is high at the surface, but decreases to background levels after the first sputter cycle. Background levels result from residual O of the analytical chamber being adsorbed between cessation of sputtering and analysis. After 30 h of air exposure the O-enriched overlayer is <10 Å thick (3 or fewer monolayers). As is enriched in the near-surface relative to pristine NiAs (Fig. 4b). Profiles of pristine surfaces gave no indication of preferential sputtering of As relative to Ni. The high near-surface As/Ni ratio likely is induced by surface oxidation, just as observed for oxidized arsenopyrite and GaAs (Nesbitt et al. 1995; Flinn and McIntyre 1990).

Water-reacted surface

The Auger compositional depth profile of NiAs reacted with distilled water for 7 d (Fig. 4c) displays a Ni:As ratio of close to 1:1 at depths greater than 140 Å, indicating pristine, unreacted niccolite. The near-surface region has high, near-constant O content and lower Ni and As contents, with Ni:As:O atomic proportions near 3:2:5. The proportions are similar to those expected of Ni-arsenite ($Ni_3[AsO_3]_2$) or Ni-arsenate ($Ni_3[AsO_4]_2$). The As(3d) XPS spectrum reveals both As^{3+} and As^{5+}. Niccolite quickly alters to annabergite (nickel bloom) in humid natural environments (Hurlbut 1961) and the salt is classified as insoluble (Weast et al. 1984), suggesting that Ni-arsenate or Ni-arsenite salts have accumulated at the surface. Although the Auger depth profile of the oxidized overlayer indicates a composition similar to Ni-arsenite or Ni-arsenate, the interpretation is suspect in that the Ni(2p) and O(1s) XPS spectra suggest that $Ni(OH)_2$ is also present in the overlayer, and that much of the O is as H_2O rather than as O^{2-} or OH^- such as is expected in the salts.

Niccolite was also reacted with distilled, deionized water for 16 h. Auger compositional depth profiles of the reacted surface indicated Ni:As:O to be about 32:23:45 at the reacted surface. The O signal decreased to 10% at 10 Å depth and to background values (about 3%) at 15 Å depth. The O enriched overlayer was consequently no more than 10 Å (3 to 4 monolayers) thick after 16 h reaction.

Surface states, As, and S reactivity at fracture surfaces

Arsenic hybridization at fracture surfaces

There are no synchrotron studies of niccolite where the photon energy was tuned to identify surface Ni or As contributions. There are, however, such studies of pyrite and GaAs, and information for these surfaces has been used to help develop a qualitative understanding of NiAs surface properties.

GaAs {110} cleavage surface. GaAs displays zincblende structure with As being sp^3 hybridized and tetrahedrally coordinated (Harrison 1980; Spicer et al. 1977; Duke et al. 1976). Bond scission resulting from cleavage along {110} surfaces yields non-saturated, dangling bonds on Ga and As surface ions. Top of valence band electrons (derived primarily from nonbonding Ga orbitals) are transferred to acceptor levels in the As valence band. This leads to sp^3 hybridization of surface As ions with a saturated dangling bond containing a lone pair of electrons and three hybrid orbitals directed toward underlying bulk Ga ions, as shown in Figure 5a (Gibson and LaFemina 1996; Harrison 1973, 1980, 1981; Spicer et al. 1977; Duke et al. 1976).

Surface relaxation also occurs whereby As protrudes from, and Ga is drawn toward, the {110} surface (Harrison 1980; Gibson and LaFemina 1996). Spicer et al. (1977) argued that each orbital containing a lone pair of electrons gained s character during fracture and the three As hybrid orbitals directed toward bulk Ga ions gain p character. This leads to contraction of the tetrahedral angle toward 90° causing the surface As ion to be pushed away from the surface and the Ga ion to be drawn toward the surface.

An alternative explanation for surface relaxation is based on the analogy of surface As ions with sp^3 hybridized nitrogen (same group as As) of NH_3 molecules. A tenet of the valence shell electron pair repulsion (VSEPR) theory is that the contraction of the H-N-H tetrahedral bond angles (109.48°) toward 90° results from repulsion of the three hybrid orbitals (directed toward H ions) by the orbital containing the lone pair of electrons. The theory can be applied to sp^3 hybridized surface As ions. Repulsion by the lone pair of electrons of the dangling bond causes contraction of Ga-As-Ga tetrahedral angles, forcing As surface ions to protrude from the fracture surface (Figs. 5a and 5c).

NiAs fracture surfaces. The electronegativity of Ni^{2+} and Ga^{3+} are, respectively, 1.75 and 1.82 by the Pauling definition (Allred 1961), but are reversed (1.91 and 1.81) by the Allred-Rochow definition (Allred and Rochow 1958). Their electronegativities are consequently similar. Just as for scission of Ga-As bonds in GaAs, rupture of Ni-As bonds in NiAs should result in transfer of electrons from the conduction band to acceptor levels in the As valence band to form lone pairs of electrons resident in dangling bonds of surface As ions.

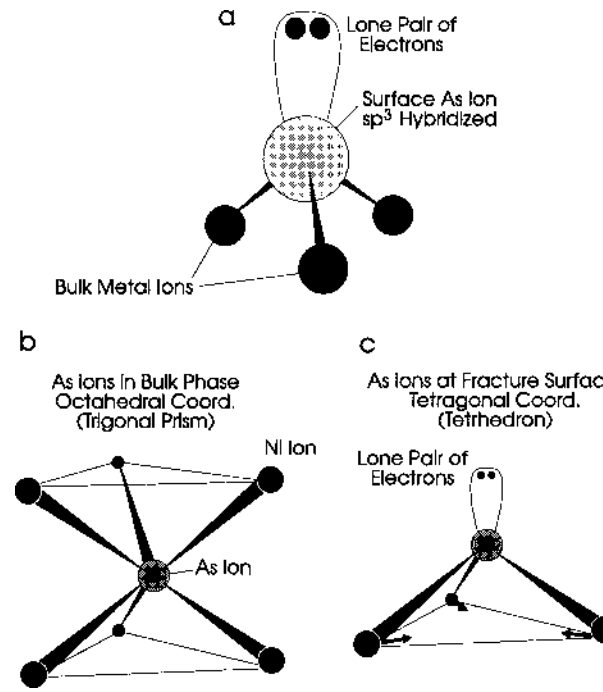

Figure 5. Schematic diagrams of As ions in bulk and surface environments of NiAs. (**a**) An sp^3-hybridized As surface ion bonded to three subtending metal ions (e.g., Ga or Ni), with the fourth hybrid bond containing a lone pair of electrons extended away from the solid surface and toward potential adsorbates. Attachment of an adsorbate results in tetrahedral coordination of the surface As ion. (**b**) A bulk As ion octahedrally coordinated to Ni ions in a trigonal prismatic arrangement. (**c**) A sp^3 hybridized As surface ion bonded to three subtending metal ions (e.g., Ga or Ni). The arrows shown on the trigonal base illustrates the contraction of bond angles resulting from repulsion of the lone pair of electrons according to the valence shell electron pair repulsion (VSEPR) theory. Such repulsion should result in protrusion of surface As ions from the surface.

Arsenic ions of niccolite are coordinated to six Ni ions as trigonal prisms (Fig 5b). Where only one or two Ni-As bonds are severed, the surface As ion remains severely constrained by the remaining Ni-As bonds. These surface As ions may retain their six hybrid orbitals through creation of one or two dangling bonds, each containing a lone pair of electrons. The VSEPR theory, however, requires each lone pair to repel all other hybrid orbitals leading to two scenarios. The trigonal prism may be distorted by contraction of Ni-As-Ni angles to minimize repulsion. Alternatively, there is minimal distortion of Ni-As-Ni bond angles, and the lone pair of electrons consequently acquire a very high energy because of their close proximity to the other hybrid orbitals. Either scenario is likely to produce a high energy surface at which relaxation or reconstruction will occur.

Where three Ni-As bonds are severed during fracture, surface As ions may adopt sp^3 hybridization, thus minimizing repulsion among hybrid orbitals. Three hybrid bonds are directed to three subtending Ni ions and the fourth (a dangling bond containing a lone pair) is directed away from the surface (Fig. 5a). This arrangement is likely to be more stable than a fivefold coordinate As surface ion with one dangling bond, or a fourfold coordinate surface ion with two dangling bonds because it would lead to dramatically lower surface bond density and lower surface energy. Formation of sp^3 hybridized As ions should be energetically favored at niccolite fracture surfaces.

These arguments, and the GaAs studies, suggest that many niccolite As surface ions are sp^3 hybridized, with one lone pair of electrons constituting the dangling bond. Even though comparatively stable, lone pair repulsion of the three hybrid orbitals directed toward subtending Ni ions (Fig. 5c) is likely to result in contraction of bond angles, pushing As away from the mineral surface and drawing Ni toward it. The sp^3 hybridized As ions on niccolite surfaces consequently should have surface properties similar to As ions at GaAs surfaces.

As and S polymerization at surfaces

The nature of surface reconstruction is specific to the surface exposed and to the composition of the face. Reconstruction of the {001} surface of GaAs results in formation of As dimers (As_2) whereby two As surface ions, each with a dangling bond, are paired (bonded) thus eliminating half the dangling bonds and thereby reducing the free energy of the surface (Biegelsen et al. 1990a). Dimers are more stable on some GaAs surfaces than are two separate As ions each with an associated dangling bond. Biegelsen et al. (1990b) also demonstrated that As trimers (As_3) form on other cleavage faces of GaAs. The necessarily complex fracture surface of niccolite is likely to include faces which have the orientation and composition required for development of As dimers and trimers. This is made more likely by the compositional layering of niccolite. Ni and As are restricted to specific planes parallel to {100}. Some surfaces therefore will be enriched in As relative to Ni. These surfaces may achieve greater stability where sp^3 hybridized As ions react to produce dimers and trimers, just as observed on the GaAs surfaces (Pashley et al. 1988; Biegelsen et al. 1990a; Biegelsen et al. 1990b). By analogy with polysulfides, these As polymeric species should yield photopeaks intermediate between As^{1-} and As°, thus contributing to the high energy side of the As^{1-} peak.

NiS, FeS_{1-x}, and $(Ni,Fe)_9S_8$ fracture surfaces

Pyrrhotites and the high temperature form of NiS display NiAs structure (or derivative structure) so that S of these phases is sixfold coordinate (Kjekshus and Pearson 1964). The arguments previously presented for As sp^3 hybridization at NiAs surfaces consequently should apply to surface sulfur atoms of the above-mentioned minerals. If so, some (if not most) surface S will exhibit sp^3 hybridization and surface relaxation is likely to result in protrusion of S ions from the surface and collapse of metal ions toward the surface. Like surface As of NiAs, sp^3 hybridized surface S ions, with lone pairs directed away from the mineral surface, are poised to react with adsorbents, and in doing so to assume tetrahedral coordination. Sulfur of monoclinic pyrrhotite, millerite (low temperature form of NiS) and pentlandite, although structurally more complex than those with NiAs structure, are also likely to assume sp^3 hybridization at fracture surfaces. The arguments are likely to apply to sulfur at these surfaces as well.

Again by analogy with GaAs surfaces, parting surfaces of NiS phases, pyrrhotites, and pentlandite enriched in S are likely to yield dimers and trimers (polymeric species) through reconstruction. There is evidence for sulfur polymers at pyrrhotite surfaces (Pratt et al. 1994a; 1994b; Pratt and Nesbitt 1997).

Incipient oxidation of NiAs surfaces

Sorption of oxygen

NiAs surface exposure to gases of the analytical chamber was approximately 4 Langmuirs before collection of the oxygen spectrum. The broadscan yields about 8.6% oxygen. After consideration of photoelectron attenuation (Briggs and Seah 1990), no more than about 8 monolayers were sampled so that the surface monolayer represents about 1/8 of atoms sampled. The surface layer should, however, contribute more than one-eighth (12.5%) of the total broadscan signal considering attenuation of signal from the deeper layers. These considerations suggest that there is sub-monolayer coverage of the fractured niccolite by oxygen-bearing species.

The O(1s) photopeak at 528.0 eV was not observed on pyrite, arsenopyrite, pyrrhotite, or millerite surfaces (Legrand et al. 1998; Knipe et al. 1995; Nesbitt et al. 1995; Nesbitt and Muir 1994; Pratt et al. 1994a, 1994b). Barteau and Madix (1984) and Joyner and Roberts (1979) observed a peak at 528.3 eV attributed to an adsorbed atomic oxygen radical [·O(ad)]. The gases of the analytical chamber are the likely source of the species in that atomic oxygen was observed in the mass spectrum of the residual gases in the reaction chamber of the XPS instrument (Nesbitt and Muir 1994; Knipe et al. 1995). Molecular oxygen may be dissociated (perhaps by the action of the vacuum pumps) or possibly it is dissociated after alighting on the mineral surface.

Barteau and Madix (1984) demonstrated that ·O(ad) reacts with H_2O(ad) to produce ·OH(ad):

$$H_2O(ad) + \cdot O(ad) \rightarrow 2\cdot OH(ad) \quad (1)$$

They also note that ·OH(ad) is located at 1.1 eV higher binding energy than ·O(ad). The ·OH(ad) radical should therefore be located at 529.1 eV of Figure 1d. Its absence may result

from rapid acquisition of an electron (from the solid) to produce OH^- at 530.9 eV. Alternatively, reaction 1 is strongly inhibited, but this second possibility seems unlikely in that both H_2O(ad) and ·O(ad) are present at the surface, and radicals generally are highly reactive. Much of the OH^- observed on the surface consequently may have formed by reaction 1.

Evidence for an As-O redox reaction

The Ni(2p) spectrum (Fig. 1a) shows no indication of Ni oxidation or reduction but the As(3d) spectrum includes small amounts of As^{1+} and As^{3+}. Arsenic of NiAs has therefore acted as a reductant. Arsenic was similarly observed to act as reductant during oxidation of GaAs by molecular oxygen (Spicer et al. 1976; 1977). Arsenic oxidation, represents a half-reaction and the other half remains to be identified. Oxygen of H_2O is fully reduced and cannot act as oxidant (e.g., dissociation of H_2O to produce OH^- does not explain the oxidized As species). H^+ of water may act as oxidant if reduced to H°. There is no evidence that this proceeds to any extent at the surface of NiAs or other common arsenide or sulfide surfaces. The most likely oxidant (the ultimate sink for electrons) is molecular oxygen of the chamber gases (perhaps via ·O[ad]). The evidence for O_2 as oxidant is, however, circumstantial and is derived from the extensive study of O_2 reaction with GaAs surfaces (Hughes and Ludeke 1986; Monch 1986; Spicer et al. 1976: 1977).

Monch (1986) showed that, at room temperature, the initial uptake of molecular oxygen (O_2) on the GaAs {110} surface was via dissociative chemisorption. Unfortunately the O_2(ad) signal, located between 530 and 532.5 eV (Barteau and Madix 1984), cannot be separated from those of H_2O and OH^- in Figure 1d. The presence of sp^3 hybridized As on both NiAs and GaAs surfaces, and the presence of ·O(ad) on NiAs surfaces (Fig. 1d) suggests that, just as on GaAs surfaces, O_2 undergoes dissociative chemisorption on NiAs surfaces. Once adsorbed, ·OH(ad) may be produced by reaction with adsorbed H_2O (Rxn. 1) and react with As to produce As(OH) and $As(OH)_3$ surface species. Formation of As(OH) may involve sp^3 hybridized As, with the As-OH bond replacing the lone pair of electrons (Fig. 5c) to produce a tetrahedrally coordinated surface As moiety. The $As(OH)_3$ surface species may be a response toward formation of a more stable sixfold-coordinated surface As moiety akin to its coordination in the bulk. The three OH^- groups bonded to surface As then should form a trigonal face extended away from the bulk; the three As-Ni bonds remain in tact, binding As to the bulk (Fig. 5b).

Oxidation of NiAs surfaces by air

Comparison of the vacuum fractured and the 30 h air-oxidized spectra (Figs. 1 and 2) indicates $Ni(OH)_2$, arsenite (AsO_3^{3-}), and arsenate (AsO_4^{3-}) in the near-surface. Air oxidation of millerite yielded equivalent species, ($Ni[OH]_2$ and $NiSO_4$, Legrand et al. 1998), hence analogous species were produced on each surface. The O(1s) spectrum of air-oxidized millerite displayed no oxide (O^{2-}) peak (530 eV) suggesting that the $Ni(OH)_2$ surface species contains no oxide component. There is oxide (O^{2-}) in arsenate ($AsO[OH]_3$), and the oxide (O^{2-}) peak of Figure 2c may arise from it.

Studies of O_2-GaAs interactions (Monch 1986; Spicer 1977) indicate that only after high O_2 dosages did more than a few monolayers of oxide accumulate at the surface. Apparently, NiAs reacts similarly in that no more than three monolayers of oxidized material accumulated at it surface after 30 h of air exposure (Fig. 4a).

The first monolayer of oxygen probably is deposited on NiAs surface via dissociative chemisorption of O_2(g). The argument is supported both by the presence of ·O[ad] on NiAs surfaces fractured in the analytical chamber (Fig. 1d), and by the analogy with oxygen uptake on GaAs surface. Continuing the analogy with GaAs, additional oxide/hydroxide overlayers accumulate through adsorption of O_2 onto the previously formed oxidized overlayer. The adsorbed O_2 is then reduced via the Mott-Cabrera mechanism (Monch 1986) whereby electrons tunnel from the NiAs surface through the previously formed contaminant oxygen layers to the outermost contaminant layer (Monch 1986; Fromhold 1976). From a band model perspective, electron transfer proceeds from the conduction band, through the oxide overlayers (tunnelling) to the electron-affinity level of O_2(ad) on the surface-most oxide layer. The rate of production of surface oxide layers necessarily decreases over time due to an increasingly thick oxide layer through which conduction band electrons must tunnel. The Auger data (Fig. 3a) confirm that oxide layer buildup is substantially slowed well before 30 h exposure to air. After 30 h a surface has been produced that is largely passivated with respect to oxidation by molecular oxygen. Presumably there is simultaneous adsorption of H_2O and O_2 so that reaction 1 proceeds to the right, producing the OH^- required to form As(OH), $As(OH)_3$ (H_3AsO_3), and $AsO(OH)_3$ (H_3AsO_4).

Because Ni and As are non-volatile, the high As/Ni ratio observed in the near-surface by Auger spectroscopy (Fig. 4b) must be a response to surface oxidation. The high ratio may result either from preferential diffusion of As toward the surface, or preferential diffusion of Ni toward the bulk. Diffusion of As toward oxidized surfaces has been observed for arsenopyrite and GaAs (Nesbitt et al. 1995; Flinn and McIntyre 1990), and outward diffusion of As probably occurs in the near-surface of NiAs. This occurs because oxidation of As^{1-} at the surface decreases its surface concentration, thereby establishing a chemical potential gradient (between surface and bulk) down which As diffuses. The near-surface consequently becomes enriched in As relative to Ni (Fig. 4b). A consequence is that the oxidized overlayer grows outward from the original NiAs surface (Nesbitt and Muir 1998).

There is consequently good evidence for diffusion of both electrons and As to the surface of the oxidized overlayer. It is uncertain whether electron or As diffusion limits outward growth of the oxide overlayer (after formation of a few monolayers). In addition, diffusion of As° through the overlayer followed by its oxidation at the surface supplies both electrons and As to the surface. If As° is produced in the subsurface (after establishment of a thin oxidized overlayer), its diffusion may be rapid (a neutral moiety) thus displacing the Mott-Cabrera and As^{1-} diffusion processes as the rate limiting process for production of oxidized overlayers. Additional studies are required to address these possibilities.

OXIDATION OF NiAs SURFACES BY AERATED WATER

NiAs reacted with aerated distilled water for 16 h and 7 d developed overlayers containing Ni-hydroxide, arsenate, and arsenite, as demonstrated by Auger compositional depth profiles (Fig. 4c) and XPS spectra (Fig. 3). The layer was no more than about 10 Å thick after 16 h reaction, and about 120 Å thick after 7 d of reaction. The results suggest growth was about 15 Å per day. Three Auger depth profiles were collected of different locations on the reacted surface. They indicated overlayer thicknesses between 100 and 150 Å and the overlayer compositions were similar to that shown in Figure 4c. The Auger-derived Ni:As:O proportions of the secondary overlayer were about 3:2:5, which is consistent with $Ni_3(AsO_3)_2 \cdot nH_2O$ or $Ni_3(AsO_4)_2 \cdot nH_2O$ (especially with regard to the Ni:As ratio). The Auger profiles and compositions suggest a compositionally homogeneous overlayer about 120 Å thick has developed on NiAs during 7 d reaction with aerated, distilled water.

The interpretation seems to conflict with the XPS data. The O(1s) spectrum reveals OH^-, whereas the Ni(2p) and As(3d) spectra indicate $Ni(OH)_2$ and As^{1-}, respectively. OH^- and As^{1-} are absent from the above-mentioned salts, and if $Ni(OH)_2$ is present in the overlayers analyzed by the Auger technique, then the reported Ni:As:O proportion are fortuitously close to the Ni-As salts in all three profiles.

The Auger and XPS data may, however, be reconciled in that the Auger data analyses micrometer diameter areas whereas the XPS data are collected from millimeter square areas. If the Ni-arsenite and arsenate salts are developed as patches over the surface (e.g., crystallite aggregates) the Auger technique may have analyzed these. Where crystallite aggregates are absent, a thin continuous $Ni(OH)_2$ overlayer may have developed that is virtually devoid of arsenite or arsenate and As^{1-} may be detected from the underlying bulk NiAs. There is good circumstantial evidence for this scenario. This precise situation was observed on millerite surfaces oxidized by air for one year (Legrand et al. 1998). $NiSO_4$ crystallites have developed as patches dispersed across the millerite surface. There is also developed a thin, continuous $Ni(OH)_2$ veneer beneath which bulk, unoxidized NiAs is detected by XPS analyses.

The water reacted NiAs surface consequently may be entirely analogous to the air oxidized NiS surface. Whereas Ni-arsenate salts are classified as insoluble (Weast et al. 1984), Ni-sulfate salts are highly soluble, hence sulfate salts are not observed on NiS water-reacted surfaces. The nature of the water reacted NiAs surface is being investigated in greater detail.

ACKNOWLEDGMENTS

This communication has benefited from discussions with D. Legrand and G.M. Bancroft and has benefited greatly from two reviews, one of which was by D. Vaughan. The research was conducted at Surface Science Western laboratories. The analytical expertise of Jay Mycroft was invaluable. We are grateful to S. McIntyre and R. Davidson for allowing ready access to the instruments. Support for the research was provided by the National Science and Engineering Research Council of Canada.

REFERENCES CITED

Allred, A.L. (1961) Electronegativity values from thermochemical data. Journal of Inorganic and Nuclear Chemistry, 17, 215–221.

Allred, A.L. and Rochow, E.G. (1958) A scale of electronegativity based on electrostatic force. Journal of Inorganic and Nuclear Chemistry, 5, 264–268.

Barteau, M.A. and Madix, R.J. (1984) A photoelectron spectroscopic investigation of the interaction between H_2O and oxygen on Ag(110). Surface Science, 140, 108–122.

Biegelsen, D.K., Swartz, L.-E., and Bringans, R.D. (1990a) GaAs epitaxy and heteroepitaxy: a scanning tunneling microscopic study. Journal of Vacuum Technology, A8, 280–283.

Biegelsen, D.K., Bringans, R.D., Northrup, J.E., and Swartz, L.-E. (1990b) Reconstructions of GaAs(111) surfaces observed by scanning tunneling microscopy. Physical Review Letters, 65, 452–455.

Briggs, D. and Seah, M.P. (1990) Practical Surface Analysis. Volume 1: Auger and X-ray Photoelectron Spectroscopy (2nd edition), 657 p. Wiley, New York.

Doniach, S. and Sunjic, M. (1970) Many-electron singularity in X-ray photoemission and X-ray line spectra from metals. Journal of Physics C: Solid State Physics, 3, 285–291.

Duke, C.B., Lubinskey, A.R., Lee, B.W., and Mark, P.J. (1976) Atomic geometry of cleavage surfaces of tetrahedrally coordinated compound semiconductors. Journal of Vacuum Science and Technology, 13, 761–768.

Eastman, D.E., Chiang, T.-C. Hermann, P., and Himpsel, F.J. (1980) Surface core-level binding-energy shifts for GaAs (110) and GaSb (110). Physical Review Letters, 45, 656–659.

Flinn, B.J. and McIntyre, N.S. (1990) Studies of the UV/ozone oxidation of GaAs using angle-resolved X-ray Photoelectron Spectroscopy. Surface and Interfacial Analysis, 15, 19–26.

Fromhold, A.T. (1976) Theory of Metal Oxidation. North-Holland, Amsterdam.

Gibson, A.S. and LaFemina, J.P. (1996) Structure of Mineral Surfaces. In P.V. Brady, Ed., Physics and Chemistry of Mineral Surfaces, 368 p. CRC Press, Boca Raton.

Harrison, W.A. (1973) Bond-orbital model and the properties of tetrahedrally coordinated solids. Physical Reviews, B8, 4487–4498

——(1980) Electronic Structure and the Properties of Solids, 582 p. Freeman, San Francisco.

——(1981) New tight-binding parameters for covalent solids obtained using Louie peripheral states. Physical Reviews, B24, 5835–5843.

Hughes, G. and Ludeke, R. (1986) O 1s studies of the oxidation of InP(110) and GaAs(110) surfaces. Journal of Vacuum Science and Technology, B4, 1109–1114.

Hurlbut, C.S. Jr. (1961) Dana's Manual of Mineralogy, 609 p. Wiley, New York.

Joyner, R.W. and Roberts, M.W. (1979) A study of the adsorption of oxygen on silver at high pressure by electron spectroscopy. Chemical Physics Letters, 60, 459–462.

Kjekshus, A. and Pearson, W.B. (1964) Phases with the nickel arsenide and closely related structures. In H. Reiss, Ed., Progress in Solid State Chemistry, p. 83–174. Macmillan Company, New York.

Knipe, S.W., Mycroft, J.R., Pratt, A.R, Nesbitt, H.W., and Bancroft, G.M. (1995) X-ray photoelectron spectroscopic study of water adsorption on iron sulfide minerals. Geochimica Cosmochimica Acta, 59, 1079–1090.

Laajalehto, K., Kartio, I., Kaurila, T., Laiho, T., and Suoninen, E. (1996) Investigation of copper sulfide surfaces using synchrotron radiation excited phtoemission spectroscopy. In H.J. Mathieu, B. Reihl, and D. Briggs, Eds., European Conference on Applications of Surface and Interface Analysis ECASIA 1995, p. 717–720. Wiley, Chichester, U.K.

Legrand, D.L., Nesbitt, H.W., and Bancroft, G.M. (1998) X-ray photoelectron spectroscopic study of a pristine millerite (NiS) surface and the effect of air and water oxidation. American Mineralogist (in press).

Mansour, A.N. (1996a) Characterization of β-$Ni(OH)_2$ by XPS. Surface Science Spectra, 3, 239–246.

——(1996b) Characterization of NiO by XPS. Surface Science Spectra, 3, 231–238.

Mansour, A.N. and Melendres, C.A. (1996a) Characterization of $Ni_2O_3 \cdot 6H_2O$ by XPS. Surface Science Spectra, 3, 263–270.

——(1996b) Characterization of γ-NiOOH by XPS. Surface Science Spectra, 3, 263–270.

McIntyre, N.S. and Cook, M.G. (1975) X-ray photoelectron studies on some oxides and hydroxides of cobalt, nickel and copper. Analytical Chemistry, 47, 2208–2213.

Monch, W. (1986) On oxidation of III-V compound semiconductors. Surface Science, 168, 577.

——(1995) Semiconductor Surfaces and Interfaces, 2nd edition, 442 p. Springer, Berlin.

Nesbitt, H.W. and Muir, I.J. (1994) X-ray photoelectron spectroscopic study of a pristine pyrite surface reacted with water vapour and air. Geochimica Cosmochimica Acta, 58, 4667–4679.

Nesbitt, H.W., Muir, I.J., and Pratt, A.R. (1995) Oxidation of arsenopyrite by air and air-saturated, distilled water, and implications for mechanism of oxidation. Geochemica Cosmochimica Acta, 59, 1773–1786.

Pashley, M.D., Haberen, K.W. Friday, W., Woodall, J.M., and Kirchner, P.D. (1988) Structure of GaAs(001) (2x4)-c(2x8) determined by scanning tunneling microscopy. Physical Review Letters, 60, 2176–2179.

Pratt, A.R. and Nesbitt, H.W. (1997) Pyrrhotite leaching in acid mixtures of HCl and H_2SO_4. American Journal of Science, 297, 807–828.

Pratt, A.R., Muir, I.J., and Nesbitt, H.W. (1994a) X-ray photoelectron and Auger electron spectroscopic studies of pyrrhotite and mechanism of air oxidation. Geochimica Cosmochimica Acta, 58, 827–841.

Pratt, A.R., Nesbitt, H.W., and Muir, I.J. (1994b) Generation of acids from mine waste: oxidative leaching of pyrrhotite in dilute H_2SO_4 solutions at pH 3.0. Geochimica Cosmochimica Acta, 58, 5147–5159.

Scofield, J.H. (1976) Hartree-Slater subshell phtoionization cross-sections at 1254 and 1487 eV. Journal of Electron Spectroscopy and Related Phenomena, 8, 129–137.

Smit, L. and van der Veen, J.F. (1986) Determination of atomic positions in the GaSb(110) and InAs(110) surfaces by medium energy ion blocking. Surface Science, 166, 183–205.

Spicer, W.E., Lindau, I., Gregory, P.E., Garner, C.M., Pianetta, P., and Chye, P.W. (1976) Synchrotron radiation studies of electronic structure and surface chemistry of GaAs, GaSb and InP. Journal of Vacuum Science and Technology, 13, 780–785.

Spicer, W.E., Lindau, I., Miller, J.N., Ling, D.T., Pianetta, P., Chye, P.W., and Garner, C.M. (1977) Studies of surface electronic structure and surface chemistry using synchrotron radiation. Physica Scripta, 16, 388–397.

Thiel, P.A. and Madey, T.E. (1987) The interaction of water with solid surfaces: Fundamental Aspects. Surface Science, 7, 211–385.

Vaughan, D.J. and Craig, J.R. (1978) Mineral Chemistry of Metal Sulfides, 493 p. Cambridge University Press, Cambridge.

Weast, R.C., Astle, M.J., and Beyer, W.H. (1984) CRC Handbook of Chemistry and Physics, 65, I-38 p. CRC Press, Boca Raton.

MANUSCRIPT RECEIVED APRIL 7, 1998
MANUSCRIPT ACCEPTED OCTOBER 31, 1998
PAPER HANDLED BY SIMON A.T. REDFERN